

RESEARCH ARTICLE

Modulation of muscle–tendon interaction in the human triceps surae during an energy dissipation task

Amelie Werkhausen^{1,*}, Kirsten Albracht^{2,3}, Neil J. Cronin⁴, Rahel Meier⁵, Jens Bojsen-Møller¹ and Olivier R. Seynnes¹

ABSTRACT

The compliance of elastic elements allows muscles to dissipate energy safely during eccentric contractions. This buffering function is well documented in animal models but our understanding of its mechanism in humans is confined to non-specific tasks, requiring a subsequent acceleration of the body. The present study aimed to examine the behaviour of the human triceps surae muscle–tendon unit (MTU) during a pure energy dissipation task, under two loading conditions. Thirty-nine subjects performed a single-leg landing task, with and without added mass. Ultrasound measurements were combined with three-dimensional kinematics and kinetics to determine instantaneous length changes of MTUs, muscle fascicles, Achilles tendon and combined elastic elements. Gastrocnemius and soleus MTUs lengthened during landing. After a small concentric action, fascicles contracted eccentrically during most of the task, whereas plantar flexor muscles were activated. Combined elastic elements lengthened until peak ankle moment and recoiled thereafter, whereas no recoil was observed for the Achilles tendon. Adding mass resulted in greater negative work and MTU lengthening, which were accompanied by a greater stretch of tendon and elastic elements and a greater recruitment of the soleus muscle, without any further fascicle strain. Hence, the buffering action of elastic elements delimits the maximal strain and lengthening velocity of active muscle fascicles and is commensurate with loading constraints. In the present task, energy dissipation was modulated via greater MTU excursion and more forceful eccentric contractions. The distinct strain pattern of the Achilles tendon supports the notion that different elastic elements may not systematically fulfil the same function.

KEY WORDS: Achilles tendon, Energy absorption, Mechanical buffer

INTRODUCTION

The spring-like properties of elastic elements, i.e. tendinous or connective tissue, enhance the function of muscle–tendon units (MTU) of the lower limb in a variety of movements (Roberts and


Azizi, 2011). During running, the body's potential energy is converted to elastic energy, which is stored in elastic elements and released to enhance movement efficiency (Fukunaga et al., 2001; Lichtwark and Wilson, 2006). During jumping, power output is increased by a rapid release of energy stored in elastic structures during muscle contraction (Farris et al., 2016; Kurokawa et al., 2001). Hence, the temporary storage of energy in elastic structures enables the uncoupling of muscle work from joint movement.

Evidence from animal studies indicates that tasks where energy dissipation is required may also benefit from such a mechanism. Using isolated preparations of plantar flexor muscles from cats and turkeys, respectively, Griffiths (1991) and Roberts and Azizi (2010) have shown that rapid stretches of the MTU were taken up by elongation of the tendon. These *in situ* observations and subsequent *in vivo* studies have convincingly demonstrated that elastic structures provide a buffering mechanism that attenuates negative power input to the muscle. As shown during drop landings of turkeys, most of the lengthening of the MTU is taken up by tendon elongation, effectively delaying and slowing down fascicle lengthening to actively dissipate energy (Konow et al., 2012). Konow and Roberts (2015) attributed this mechanism to the double advantage of constraining the muscle to a favourable operating length and to a safer lengthening velocity. Despite the importance of such a mechanical buffer in daily activities where deceleration is required (e.g. walking down stairs or downhill, dropping from a ledge), energy dissipation does not seem to have been investigated systematically in humans.

A few studies have provided insight into the role of muscle and elastic elements when energy is dissipated in the human lower leg during locomotor tasks. These movements typically involve an initial deceleration of the body, followed by an acceleration in a different direction (e.g. countermovement jumps and stair descent). Kawakami et al. (2002) found that, during the ankle dorsiflexion phase of a countermovement jump, gastrocnemius fascicles were passively lengthened for a short time before contracting isometrically, whereas the MTU lengthened. During stair descent, Spanjaard et al. (2007) reported that the fascicles of the gastrocnemius muscle shortened at first when ground reaction force (GRF) increased and lengthened thereafter throughout the single-support phase, whereas the MTU acted relatively isometrically. Thus, the deceleration required in these examples results in an uncoupling of muscle fascicle behaviour from that of the MTU, consistent with the buffering mechanism shown in animal studies. However, the subsequent acceleration inherent in such movements implies complex muscle–tendon behaviour, whereby energy is partly dissipated and partly recycled to limit muscle work or to enhance mechanical power during the push-off phase. For instance, the relatively low muscle activity recorded during fascicle lengthening may reflect the necessity to limit energy dissipation when descending stairs. Consequently, the task of stair descent may

¹Department of Physical Performance, Norwegian School of Sport Sciences, Sognsveien 220, 0863 Oslo, Norway. ²Institute of Biomechanics and Orthopaedics, German Sport University Cologne, Am Sportpark Müngersdorf 6, 50933 Köln, Germany. ³Medical Engineering and Technomathematics, University of Applied Sciences Aachen, Bayernallee 11, 52066 Aachen, Germany. ⁴Department of Biology and Physical Activity, University of Jyväskylä, Seminaarinkatu 15, 40014 Jyväskylä yliopisto, Finland. ⁵Institute for Biomechanics, ETH Zurich, Rämistrasse 101, 8092 Zurich, Switzerland.

*Author for correspondence (amelie.werkhausen@nih.no)

 A.W., 0000-0002-3194-2282

not be optimal to investigate the role of muscle and elastic elements during energy dissipation. Additionally, the role of different elastic elements is unclear in the mentioned studies. Lichtwark and Wilson (2006) showed that, during walking and running, the strain of so-called ‘series elastic elements’ can considerably differ from that of the Achilles tendon *per se*.

Hence, the objective of this study was to investigate the behaviour of muscle, tendon and elastic elements of the lower leg during a pure energy dissipation task. During a one-legged step landing, we predicted that elastic elements would buffer the rapid stretch of the triceps surae MTU, enabling muscle fascicles to operate at a limited range and velocity, but at a higher level of muscle activity than during locomotion. The stability of this mechanism under higher requirements for energy dissipation was tested in an additional experimental condition with added mass. Assuming an increase in energy absorption requirements, we expected an increase in the strain of the fascicles and/or an increase in force, which would be reflected by increased electromyographic (EMG) activity. Based on differences in fascicle behaviour observed between the biarticular gastrocnemius and the monoarticular soleus during locomotion (Cronin et al., 2013), both muscles were included in the analysis. Being monoarticular, the soleus muscle was expected to be more affected than the gastrocnemius by increased ankle flexion under the added-mass condition and to display more pronounced changes (e.g. increases in fascicle strain and/or EMG activity). A secondary objective was to elucidate more specifically the role of the Achilles tendon during energy dissipation. As previously shown, the strain estimated during walking and running for so-called ‘series elastic elements’ (essentially Achilles tendon, aponeurosis and proximal tendon) can considerably differ from that of the Achilles tendon *per se* (Lichtwark and Wilson, 2006). We therefore measured length changes of the Achilles tendon and compared it to the calculated strain of combined elastic elements. Owing to their different mechanical properties, we expected distinctive strain patterns in the tendon and in combined elastic elements during energy dissipation, despite these structures often being referred to interchangeably.

MATERIALS AND METHODS

Subjects

Thirty-nine male athletes habitually engaged in ski jumping ($n=21$, age 23 ± 3 years, height 179 ± 6 cm and mass 64 ± 4 kg) and distance running ($n=18$, age 27 ± 5 years, height 180 ± 5 cm and mass 68 ± 6 kg) took part in this study. The two types of athletes were initially recruited for a larger project. They were merged for this study after verifying the homogeneity of their anthropometric characteristics (age 25 ± 4 years, height 179 ± 6 cm and mass 66 ± 5 kg) and the similarities of their triceps surae MTU properties. All subjects gave their written informed consent and the ethical committee of the Norwegian School of Sport Sciences approved the study.

Protocol

Resting anatomical measurements were performed prior to testing. Height, body mass and right lower leg length (between the lateral malleolus and the lateral femur epicondyle) were measured for each subject. While the subjects were lying prone with the ankle joint at 90 deg (anatomical position), ultrasound images were recorded (LS128, Telemed, Vilnius, Lithuania) to visualise the muscle architecture of the gastrocnemius medialis and soleus.

After a general warm up consisting of 5 min running on a treadmill at a self-selected speed, subjects were then asked to perform a unilateral step landing task. The task was performed from a step height adjusted to individual body mass to standardise

potential energy (240 J). Subjects were instructed to step down with their right leg whilst the left foot remained on the step to maintain balance. Five trials were performed to record ultrasound scans of the gastrocnemius medialis fascicles, and five additional trials were used to scan the gastrocnemius myotendinous junction. The size and strapping of the ultrasound probe did not allow simultaneous positioning of EMG sensors over the target muscles. For this reason, gastrocnemius, soleus and tibialis anterior EMGs were recorded from the left leg in five separate trials. The 15 landing trials were conducted twice, once with body mass only and once with a vest loaded with 20% individual body mass.

Kinematics and kinetics

During the step landing task, motion capture (12 cameras, Qualisys, Gothenburg, Sweden) was used to record the positions of 18 reflective markers placed on the right leg and the hips. A modified Cleveland marker set was used for the right lower extremities. Markers were placed on the left and right anterior and posterior iliac spines to define the pelvis segment and hip joint centres (Bell et al., 1989). The right knee joint centre was defined as the mid-distance between the markers on the medial and lateral condyles. Likewise, the ankle joint centre was determined as the mid-point between the medial and lateral malleoli. To track the foot segment, markers were placed on the calcaneus and the metatarsals (first, second and fifth head). The thigh and shank segments were tracked with marker clusters consisting of four markers, placed mid-way on their respective lateral sides. Force data were recorded on a force plate (M-Gait, Motekforce Link, Amsterdam, The Netherlands) at a frequency of 1500 Hz.

Kinematic and kinetic data were analysed offline using a standard Newton–Euler inverse dynamics procedure (Visual 3D, C-Motion Inc., Germantown, MD, USA). Joint angles, moments and powers were expressed in the coordinate system of the respective proximal segment. Reference frames for all segments were defined during a standing reference measurement. Joint power was calculated as the product of the joint moment and the joint angular velocity. Data were filtered with a bidirectional first-order low-pass Butterworth filter with a cut-off frequency of 15 Hz (Kristianslund et al., 2012). Shank length was used in combination with ankle and knee joint angles to estimate MTU lengths of the gastrocnemius and soleus based on a frequently used regression equation (Hawkins and Hull, 1990). Strain velocities of MTUs were determined by differentiating their respective lengths.

Muscle–tendon behaviour

Muscle fascicles were imaged using ultrasound at a frame frequency of 80 Hz. The transducer was positioned over the gastrocnemius and soleus muscle bellies to visualize fascicles and aponeuroses. The transducer was securely fastened to the skin with adhesive tape at the interface of a custom-made holder to avoid probe movement. Fascicle length and pennation angle were analysed using a semi-automated tracking algorithm (Cronin et al., 2011; Farris and Lichtwark, 2016). Fascicle length was defined as the length between the insertions to the superficial and deep aponeuroses. Pennation angle was defined as the angle between fascicles and the deep aponeurosis for gastrocnemius, and as the angle between fascicles and the superficial aponeurosis for the soleus. The compound length of series elastic elements was calculated as follows (Fukunaga et al., 2001):

$$L_{EE} = L_{MTU} - L_f \cdot \cos \alpha, \quad (1)$$

where L_{EE} is the length of the series elastic elements, L_{MTU} is the length of the MTU, L_f is the length of the fascicle and α is the fascicle

pennation angle. Velocities were calculated as the first derivatives of MTU and fascicle lengthening.

Ultrasound scans of the gastrocnemius medialis myotendinous junction in the line of action of the muscle were used to estimate tendon length. Three reflective markers forming a triangle were rigidly attached to the ultrasound transducer, which was secured to the skin. Marker positions were synchronously recorded with the Qualisys motion-capture system. The position calibration of the transducer markers in relation to the ultrasound image plane allowed the calculation of position and orientation of the ultrasound image in the three-dimensional laboratory coordinate system (Lichtwark and Wilson, 2005). The displacement of the myotendinous junction was analysed in the two-dimensional (2D) ultrasound image using Tracker software (Tracker 4.95; www.physlets.org/tracker/). Achilles tendon length was estimated as the distance between the myotendinous junction and the calcaneus marker placed over the osteotendinous junction, as determined with ultrasound scanning. All ultrasound data were filtered similarly to kinematic and kinetic data.

Electromyography

Gastrocnemius, soleus and tibialis anterior EMGs were recorded from the left leg (TeleMyo DTS, Noraxon U.S.A. Inc., Scottsdale, AZ, USA) at an acquisition frequency of 1500 Hz. Electrode positioning and skin preparation were performed according to the SENIAM guidelines (Hermens et al., 2000). Data were treated offline with a bidirectional high-pass Butterworth filter with a cut-off frequency of 20 Hz. After rectifying, the signal was filtered with a 6 Hz bidirectional low-pass Butterworth filter (Maharaj et al., 2016). Within each subject, EMG data were normalised to the peak value reached during the step landing task without additional mass. Mean EMG values were calculated over the five trials of each subject. In some instances, one of the trials contained data points deviating from the mean by more than three times the s.d. These trials were excluded and the mean was re-calculated with the remaining four trials.

Data processing and statistical analysis

Data were reduced to the landing phase corresponding to the generation of negative ankle power and resampled to 101 data points. In the case of EMG data recorded from the left leg, kinematic data were not available to identify the phase of negative power. Therefore, the landing phase was defined for this variable by matching GRF events recorded in both legs. For all variables, the analysed phase was divided into three sub-phases based on GRF (Fig. 1): near constant force (phase 1), force rise (phase 2) and force decay (phase 3). Phase 1 started at the onset of negative ankle power and ended at the point at which the fastest change in rate of GRF development occurred (as defined by the peak of the GRF second derivative). Although force arguably increases throughout phases 1 and 2, the event closing the first phase was defined to offer an additional level of analysis because it also coincides with a change in the lengthening patterns of the MTU and its components. The subsequent phase 2 ended at the time point of peak GRF. The third phase was defined as the remaining time period, where GRF decreased.

For each subject, a multiple-correlation analysis was performed between the time–ankle-angle curves to identify atypical trials. A correlation coefficient of ≥ 0.95 was required between at least four of the trials to ensure that retained data would reflect a consistent execution of the task for each individual. Additionally, to ensure tracking quality, a coefficient of correlation above 0.90 for a given

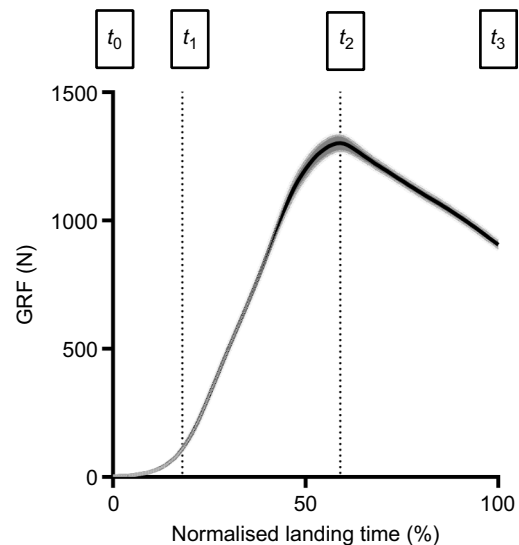


Fig. 1. Ground reaction force (GRF) during the energy dissipation task. All data were obtained between t_0 (0% normalised landing time) and t_3 (100% normalised landing time), corresponding to the onset and the end of negative ankle power, respectively. Three sub-phases [near constant force (phase 1), force rise (phase 2) and force decay (phase 3)] were determined by calculating t_1 (maximum change in rate of force development) and t_2 (peak force).

trial was required for inclusion. All data were analysed as the mean of at least four trials for each subject.

For statistical analysis, repeated measures one-way ANOVAs and Tukey's multiple comparisons were used to compare changes in length of the different MTU constituents during phases 1, 2 and 3 (t_0 to t_1 , t_1 to t_2 and t_2 to t_3 , respectively) (Prism, GraphPad Software Inc., La Jolla, CA, USA). Student's *t*-tests were performed to compare the changes in MTU and fascicle length between gastrocnemius and soleus muscles, and between ankle and knee moment and power. To analyse the influence of mass conditions (body mass versus added mass), relevant peak values and changes occurring in the three phases were compared using *t*-tests. The alpha level was set to 0.05. The data are presented as means \pm s.d. in the text, tables and boxplots, and as means \pm s.e.m. in the figures with line plots for clarity.

RESULTS

The data sets recorded during the condition with added mass had to be discarded for two subjects whose ankle kinematics data did not meet the inclusion criteria (i.e. changes in ankle joint angle differed too much between trials). In addition, the soleus ultrasound data of four subjects were removed due to insufficient quality of the images of the fascicles. Hence, the data of 39 subjects were included in the final analysis of the task with body mass, 37 subjects for the task with added mass. For the variables obtained from soleus scans (length and velocity of soleus fascicle and MTU), the number of subjects in both conditions was 35 and 33, respectively.

Kinematics and kinetics

Ankle and knee joint angle, moment and power measured during the landing phase are presented in Fig. 2. Peak moment and power normalised to body mass were higher in the ankle joint (-1.79 ± 0.29 N m kg $^{-1}$; -10.89 ± 2.36 W kg $^{-1}$) than in the knee joint (-1.33 ± 0.50 N m kg $^{-1}$, $P \leq 0.01$; -4.92 ± 3.09 W kg $^{-1}$, $P \leq 0.01$) and occurred earlier in the ankle than in the knee joint.

In the condition with added mass, ankle dorsiflexion and knee flexion were greater than in the unloaded condition. For both joints,

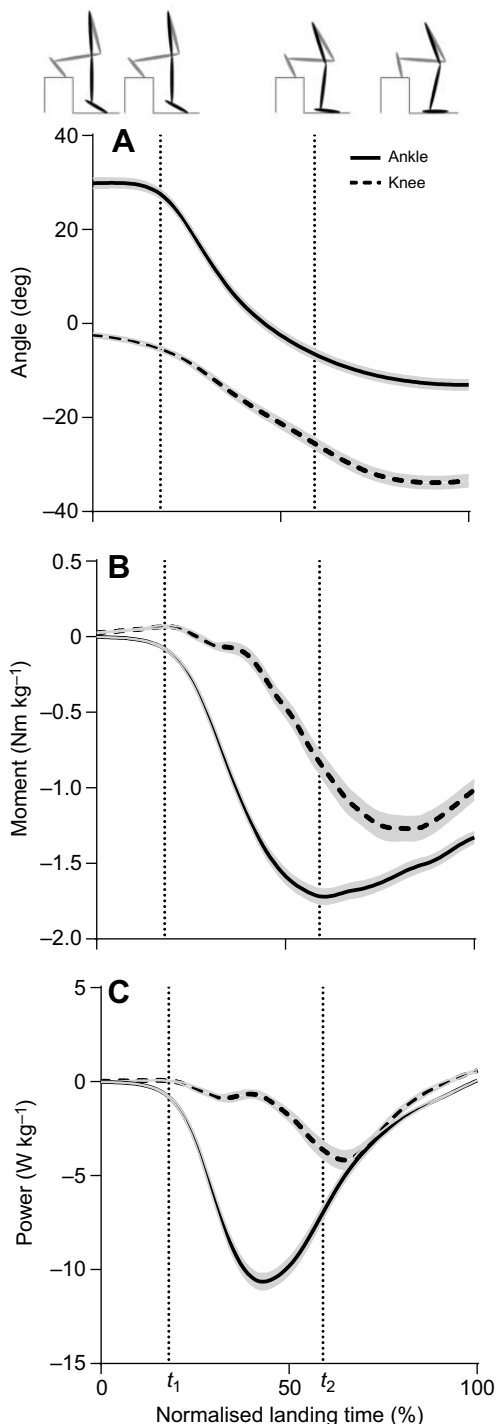


Fig. 2. Joint angle, normalised moment and normalised power at the ankle and knee joints during energy absorption in the body-mass condition. Data are means \pm s.e.m. Time series are normalised to 101 points. Negative changes in angle correspond to ankle dorsiflexion and knee flexion (0 deg corresponds to anatomical position). Moment and power are normalised to body mass. Vertical dotted lines represent the time points of the highest rate of GRF development (t_1) and peak GRF (t_2).

significantly higher peak moments and powers were produced with added mass (Fig. 3A–E). Adding mass resulted in an increase in negative work at the ankle joint from -58.06 ± 13.03 to -67.06 ± 15.08 J and the duration of the landing phase was prolonged by 10% (0.21 ± 0.02 s without, versus 0.24 ± 0.02 s with added mass).

Muscle activity

The EMG signals obtained from gastrocnemius, soleus and tibialis anterior muscles were normalised to peak values obtained during the phase of negative power, without added mass (Fig. 4). All three muscles were activated during the negative power production period. The greatest activity of gastrocnemius was seen during phase 1, whereas soleus activity increased throughout phases 1 and 2. Additional mass increased the activity of soleus and tibialis anterior, but not that of gastrocnemius (Fig. 5).

MTU measures

The mean length of the fascicles at rest was 59 ± 10 and 37 ± 10 mm for gastrocnemius and soleus, respectively. Both gastrocnemius and soleus MTUs lengthened significantly throughout the whole landing task (Fig. 6A). A greater lengthening was observed for the soleus MTU than for the gastrocnemius MTU during phase 3 (5.5 versus 4.0 mm, respectively, $P \leq 0.01$). By contrast, a larger strain was observed in gastrocnemius fascicles than in the soleus ($P \leq 0.01$ in all three phases), despite parallel changes in all phases (shortening–lengthening–lengthening). The highest lengthening velocities of gastrocnemius and soleus MTUs were reached during phase 2 (539 ± 155 and 545 ± 145 mm s⁻¹, respectively) (Fig. 7A). Unlike MTUs, gastrocnemius and soleus fascicles shortened significantly in phase 1 and lengthened during the rest of the landing (Table 1, Fig. 6B). Gastrocnemius fascicles lengthened at a faster velocity than soleus fascicles (peak velocities: 214 ± 50 and 132 ± 32 mm s⁻¹, respectively, Fig. 6B). Peak fascicle velocity occurred later than peak MTU velocity. The Achilles tendon and all elastic elements lengthened between t_0 and t_1 as well as between t_1 and t_2 . In the last phase (force decay, between t_2 and t_3), Achilles tendon length did not change significantly, whereas elastic elements shortened. Achilles tendon lengthening during phase 2 (i.e. when negative power production was highest) was relatively lower (2.9%) than that of the elastic elements as a whole (3.6%) (Table 1, Fig. 6C,D).

Adding mass to the subjects resulted in larger gastrocnemius and soleus MTU lengthening during phases 2 and 3, when GRF and ankle moment were higher (Fig. 8A,B). For the soleus MTU, a slight lengthening was also observed in phase 1, at low GRF and ankle moment levels. Length change of the Achilles tendon was significantly greater in phase 2 but not in phases 1 and 3 (Fig. 8E,F), whereas elastic element length change differed significantly between mass conditions in phases 1 and 2. Contrarily, gastrocnemius and soleus muscle fascicle lengths did not differ significantly between experiments with body mass and added mass (Fig. 8C,D).

DISCUSSION

Our results support the hypothesis of a buffering function of elastic structures enabled by a decoupling mechanism between the behaviour of the MTU, muscle fascicles and elastic structures during energy dissipation. These findings are consistent with animal studies describing the buffering and shock-absorbing function of the tendon (Konow et al., 2012), and expand on previous studies of human triceps surae behaviour during movements requiring limited energy dissipation (countermovement and stair descent). Hence, in a pure energy dissipation task as performed in the present study, stretching of elastic elements accommodates the initial lengthening of the MTU but, in contrast to other decelerating movements, energy is then quickly dissipated via early and active fascicle lengthening in both the gastrocnemius and soleus. A late recoil of combined elastic elements, but not the Achilles tendon solely, supports our hypothesis of distinct strain patterns of the two structures during energy dissipation.

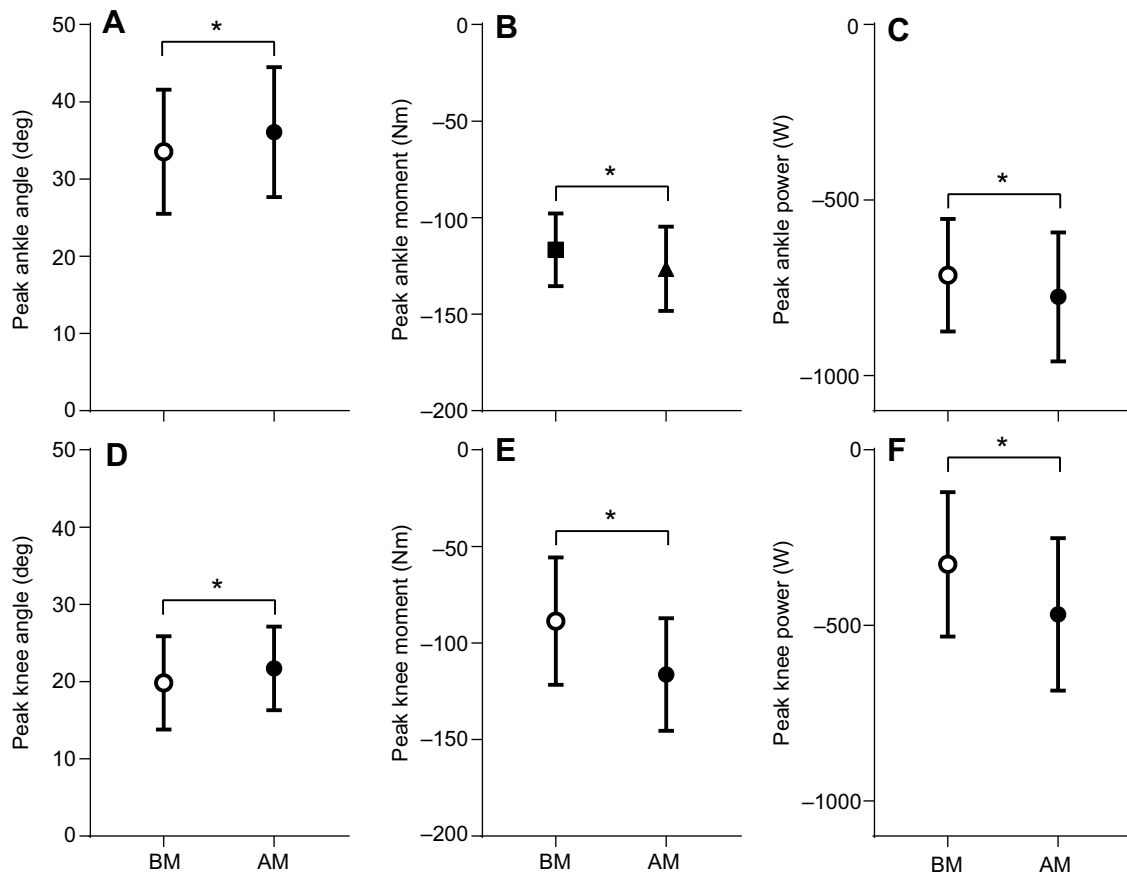


Fig. 3. Comparison of peak values of ankle and knee angle, moment and power between trials with body mass and 20% added mass during energy absorption. Data are means \pm s.d. * $P < 0.05$ when compared with the other condition. BM, body mass; AM, added mass.

The role of elastic structures in energy dissipation

At the onset of negative power, when the joint moment increased slightly, ankle dorsiflexion caused a quasi-isometric followed by a small lengthening of gastrocnemius and soleus MTUs. A concomitant stretch of the tendon and combined elastic elements

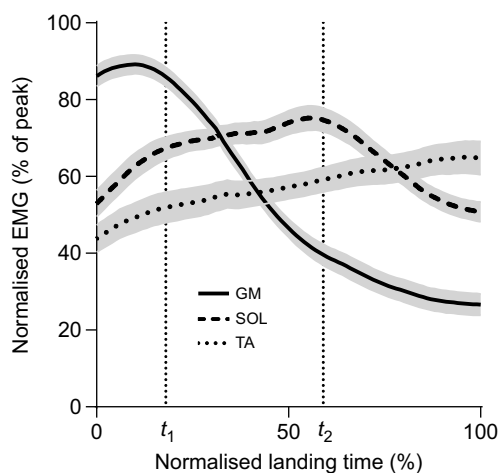


Fig. 4. Electromyographic (EMG) activity of gastrocnemius medialis (GM), soleus (SOL) and tibialis anterior (TA) during energy absorption in the body-mass condition. Data are means \pm s.e.m. Time series are normalised to 101 points. Values were normalised to peak values during the stepping-down task. Vertical dotted lines represent the time points of the highest rate of GRF development (t_1) and peak GRF (t_2).

was observed, whereas gastrocnemius and soleus fascicles shortened (Fig. 6). Energy is thus stored in elastic elements – not dissipated – at this stage and a counteracting plantar flexion moment is generated. In phase 2, characterised by the greatest increase in force, ankle dorsiflexion led to further lengthening of the MTUs. Concurrently, tendon and combined elastic elements lengthened, although to a different extent. At the increased magnitude and velocity of MTU stretch, fascicles started to actively lengthen and dissipate energy. Whereas gastrocnemius muscle activity declined, the activity of soleus peaked in this phase. However, the elongation of elastic elements enabled both gastrocnemius and soleus fascicles to lengthen at a slower rate than their respective MTUs (Fig. 7). Hence, in addition to limiting the length of active fascicles, the uncoupling between fascicles and MTU behaviour enables a delayed, slower contraction of muscle fibres. In animal studies, the mitigation of fascicle lengthening velocity has been linked to a reduction in power input to the fascicles (Konow and Roberts, 2015). We could not apply the same invasive measurements in human subjects, but power input to fascicles was likely limited here, via the buffering action of elastic elements. In support of this assumption, the delay in peak fascicle velocity during this phase enabled peak fascicle lengthening to be uncoupled from MTU stretch (Fig. 7). These findings, and the link between fascicle strain magnitude (e.g. Guilhem et al., 2016) or velocity and muscle damage, are congruent with a protective mechanism against damage. During force decay (phase 3), MTUs lengthened at a much slower rate (about 9% of peak velocity). Elastic elements shortened, whereas the length of the Achilles tendon alone did not

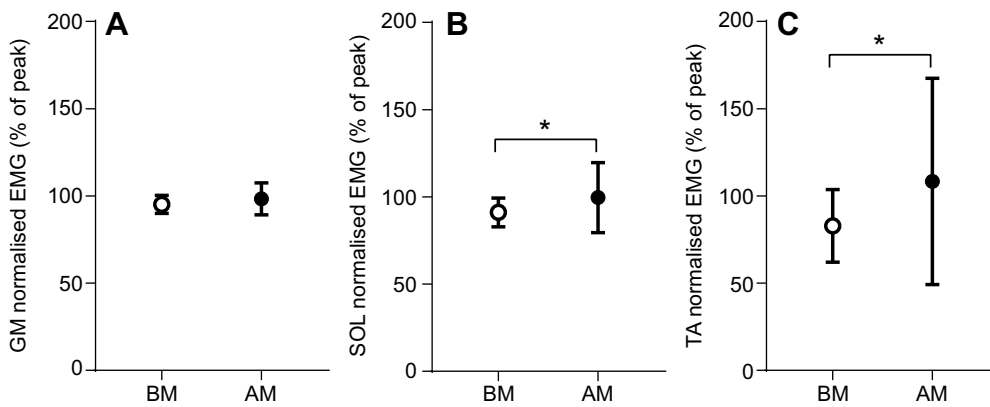


Fig. 5. Comparison of peak EMG activity occurring during energy absorption, with and without added mass. Data are means \pm s.d. Data from GM (A), SOL (B) and TA (C) muscles are normalised to peak values obtained during the entire stepping-down task. * $P < 0.05$ when compared with the other condition.

change. At the end position of the task, whereas no more negative power was produced at the ankle, the Achilles tendon was still strained by 6%, close to the maximal value recorded during the task. The different behaviour between elastic elements and the Achilles tendon highlights the importance of other elastic structures in the triceps surae MTU during energy dissipation. Besides the unknown mechanical properties of the proximal tendon, recent studies (Raiteri et al., 2016; Tilp et al., 2012) have shown the complex role of aponeuroses. Unlike tendons, the elasticity of aponeuroses does not depend on force alone and seems geared by the active state of muscles via changes in the orientation of their fibres. Changes in the pennation angle of fibres are associated with the muscle's architecture gear ratio, whereby changes in fibre length are partly dissociated from muscle – and aponeuroses – strain patterns (Azizi et al., 2008). Although not measured in the present study, the gear ratio is reportedly more important during lengthening than

shortening contractions (Azizi and Roberts, 2014) and may explain some of the differences seen between combined elastic elements and the Achilles tendon alone. Additionally, spring-like elements located in muscles (actin–myosin cross-bridges, titin and connective tissue) can store elastic energy during contraction (for a review, see Roberts, 2016). The relative contribution of these elements, in series and in parallel with the tendon, is yet unknown and future studies should establish its functional significance during decelerating movements. However, it should be noted that this difference might partly be explained by methodological reasons, owing to the different techniques and assumptions related to length measurements of these tissues. Whereas elastic element lengths were calculated based on changes in MTU length and muscle architecture, Achilles tendon length was measured directly, with the different possible sources of error such as the assumption of a 2D conformation. Regardless of these considerations, the recoil or

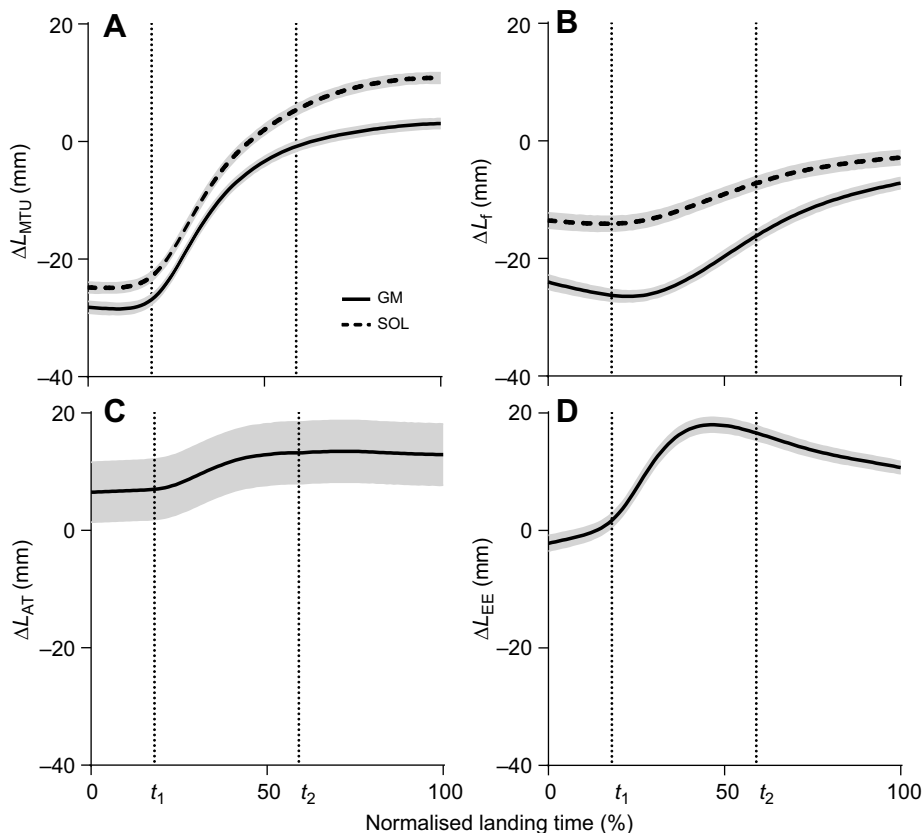


Fig. 6. Instantaneous length changes of muscle-tendon unit (L_{MTU}), fascicles (L_f), Achilles tendon (L_{AT}) and elastic elements (L_{EE}) in the unloaded condition during energy absorption. Data are means \pm s.e.m. Time series are normalised to 101 points. Data are displayed as difference to resting lengths measured when lying prone in the anatomical position. Vertical dotted lines represent the time points of the highest rate of GRF development (t_1) and peak GRF (t_2).

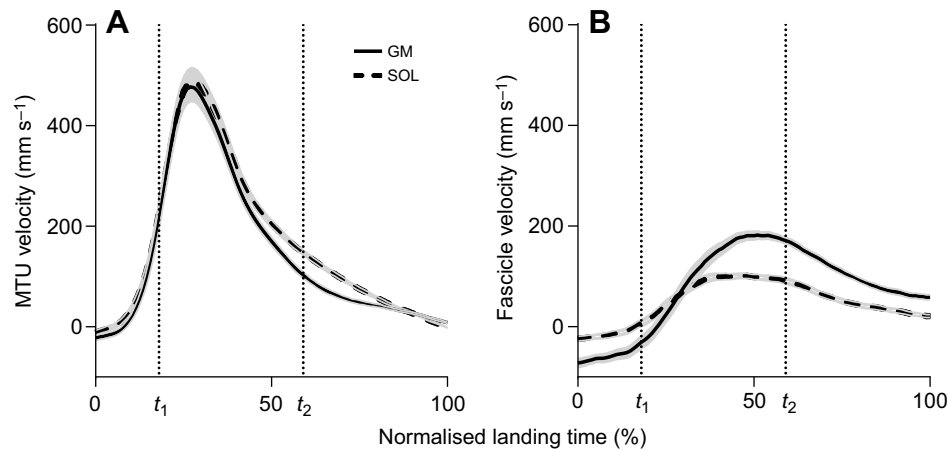


Fig. 7. Instantaneous MTU and fascicle velocity of GM and SOL during energy absorption. Data are means \pm s.e.m. Time series are normalised to 101 points. Vertical dotted lines represent the time points of the highest rate of GRF development (t_1) and peak GRF (t_2).

isometric behaviour of elastic structures during MTU lengthening drove further fascicle lengthening in phase 3. The occurrence of active fascicle lengthening during the end of the task indicates that energy was being dissipated in phase 3, despite the shortening of the MTU.

The near-constant fascicle lengthening and energy dissipation occurring during a pure energy dissipation task contrasts with previous observations from tasks requiring an acceleration of the body after ground contact. During drop jumps, for instance, gastrocnemius fascicles were found to shorten throughout the contact phase, presumably to generate and retain the elastic energy used during push-off (Ishikawa et al., 2005). Closer to our experimental model, Spanjaard et al. (2007) showed a lengthening of gastrocnemius fascicles during the single-support phase of stair descent. However, differences in the timing of changes in EMG activity and fascicle length distinguish stair descent from the energy dissipation task of the present protocol.

Contrary to our findings, fascicles were found to shorten during stair descent from touch down to nearly the end of the negative power phase. Subsequent lengthening mainly occurred when no power was being produced at the ankle joint, during the single-support phase. The relatively large fascicle shortening and the delayed fascicle lengthening during stair descent indicates that energy is dissipated more slowly and may be recycled to perform the subsequent single-support phase. This may help to regulate the optimal tension within the MTU, favouring motor control more than energy dissipation in this task. This pattern is less marked in the present task, where the sole requirement is rapid and effective energy dissipation. Albeit hypothetical, differences between step landing and stair descent tasks may reflect a regulative mechanism whereby energy in excess of that required to maintain the upright position is either dissipated or recycled towards acceleration of the centre of mass.

Effect of added mass

As expected, equipping the subjects with weighted vests increased GRF and joint moment. The increase in EMG activity of the soleus muscle, but not in the gastrocnemius, with additional load may be explained by the different insertions of the two muscles (monoarticular versus biarticular). In this condition, the greater ankle dorsiflexion caused a larger stretch of both MTUs, whereas lengthening of the biarticular gastrocnemius MTU was partly offset by the increased knee flexion. An increased co-activation of the tibialis anterior muscle probably reflected the higher torque produced by the soleus muscle. Elastic structures acted to absorb the additional work at the ankle, as illustrated by a greater stretch of the tendon and all elastic elements during phase 2 (Fig. 7H,K). Consequently, fascicle lengthening remained unchanged in the added-mass condition. Albeit speculative, the preserved fascicle strain in spite of higher negative work at the ankle may prevent strain-induced damage. Furthermore, limiting fascicle strain may prevent the muscle from operating over less advantageous regions of the force–length relationship (Katz, 1939). During phase 3, the greater lengthening of soleus and gastrocnemius MTUs caused by the added mass was not reflected by any significant difference in tendon, elastic elements or fascicle behaviour. This discrepancy may be ascribed to the larger variability of ultrasound-based measurements and the relatively small changes observed during this phase.

Overall, the increased stretch of tendon and elastic elements with added mass underlines the important role of these structures as a mechanism to control different demands of energy dissipation during human movement. This hypothesis is congruous with an earlier study examining the effects of increased demand for energy dissipation during stair descent by modulating step height (Spanjaard et al., 2008). Similarly to the added-mass condition of

Table 1. Mean length changes relative to the length at t_0 of elastic elements, Achilles tendon, and gastrocnemius medialis and soleus muscle–tendon unit and fascicles at selected time points in the unloaded condition

Time point	ΔL_{MTU} (mm)		ΔL_f (mm)		ΔL_{AT} (mm)	ΔL_{EE} (mm)
	GM	SOL	GM	SOL		
t_1	1.3 \pm 2.1*	1.9 \pm 2.1*	–2.3 \pm 2.2*	–0.5 \pm 1.2*	0.5 \pm 1.0*	3.9 \pm 2.6*
t_2	27.4 \pm 7.4*	30.2 \pm 7.3*	7.6 \pm 6.9*	6.3 \pm 3.5*	6.7 \pm 4.4*	18.7 \pm 7.9*
t_3	31.3 \pm 7.2*	35.6 \pm 7.2*	16.8 \pm 6.6*	10.6 \pm 3.2*	6.4 \pm 4.2	12.9 \pm 7.4*

Data are means \pm s.d. L_{MTU} , muscle–tendon unit length; L_f , fascicle length; L_{AT} , Achilles tendon length; L_{EE} , elastic element length; GM, gastrocnemius medialis; SOL, soleus. t_0 , onset of negative ankle power; t_1 , highest rate of ground reaction force (GRF) development; t_2 , peak GRF; t_3 , end of negative ankle power.

* P <0.05 when compared with the preceding event.

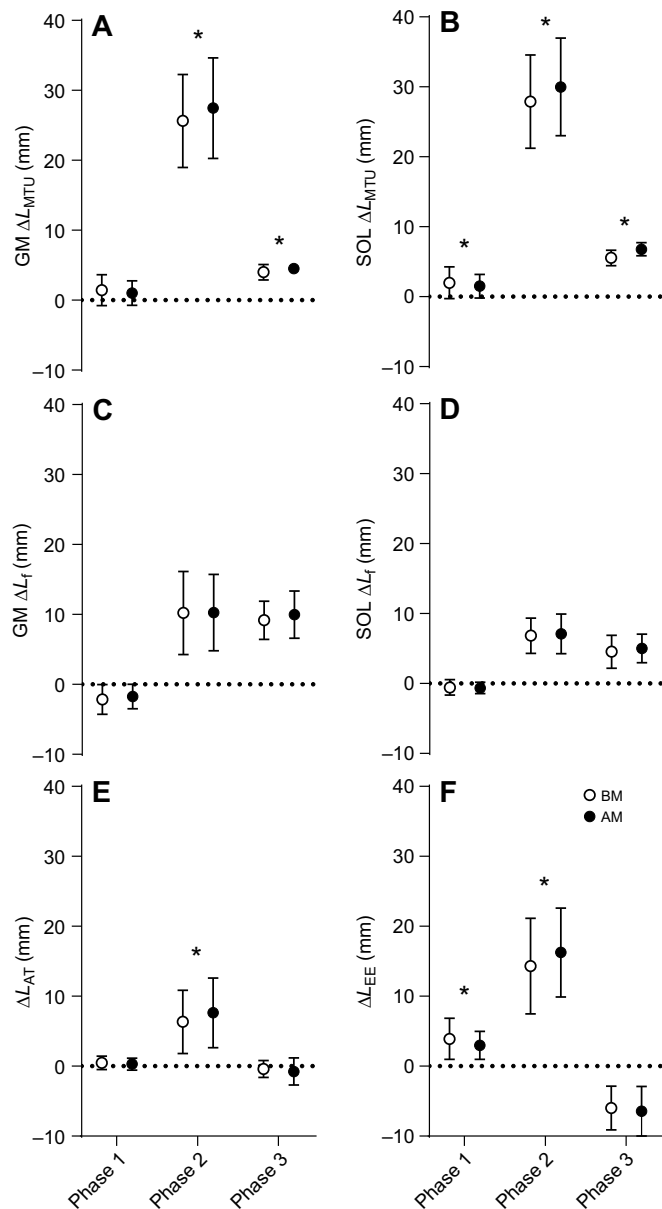


Fig. 8. Length changes of components of the MTU during the landing task, with and without added mass. Data are means \pm s.d. Sub-phases are based on GRF: near-constant force (phase 1), force rise (phase 2) and force decay (phase 3). * $P < 0.05$ when compared with the other condition.

our study, an increase in step height led to a greater stretch of elastic elements (Spanjaard et al., 2008). However, contrary to our findings, a higher demand for energy dissipation during stair descent caused an increase in fascicle shortening. In line with Spanjaard et al. (2008) and similar observations in animals by Konow and Roberts (2015), increasing body mass would be expected to induce larger fascicle shortening at the onset of the present task. Indeed, an initial shortening of fascicles allows a greater subsequent lengthening and may enable dissipation of more energy. The lack of change in fascicular behaviour with added mass may be ascribed to a different strategy of energy dissipation. As evidenced by the greater EMG activity of the soleus and the longer duration of fascicle lengthening, additional energy in the loaded condition was mainly dissipated via longer, more forceful eccentric contractions in the present task. This further suggests the central role

of muscle activation in regulating the rate of energy dissipation according to the task constraints (i.e. complete deceleration or reacceleration of the centre of mass).

Conclusion

During a task requiring energy dissipation, elastic structures of the human triceps surae buffer mechanical energy in a similar manner to that described in drop landings of animals. However, different patterns of muscle activity and fascicle lengthening found between this task and other movements involving eccentric actions suggest that this mechanism can be modulated differently, depending on the movement characteristics. The temporary storage of elastic energy is commensurate with loading constraints to limit the maximal strain and lengthening velocity of muscle fascicles. Additional energy is absorbed during a longer phase of energy absorption and seems to be dissipated via higher force production of the soleus and longer-lasting eccentric contractions. Under the present experimental conditions, the behaviour of the Achilles tendon appeared similar but not identical to that of all elastic elements, implying that the function of the two structures cannot be studied interchangeably. Finally, our results show that the pattern of fascicle lengthening during active energy dissipation is similar in the biarticular gastrocnemius and in the monoarticular soleus. However, the two muscles may contribute differently to an increased demand for energy dissipation.

Acknowledgements

We thank Cordula Schmidt for her support during the data collection.

Competing interests

The authors declare no competing or financial interests.

Author contributions

Conceptualization: A.W., K.A., N.J.C., J.B.-M., O.R.S.; Methodology: A.W., K.A., N.J.C., O.R.S.; Formal analysis: A.W., R.M.; Investigation: A.W., R.M.; Data curation: A.W., R.M.; Writing - original draft: A.W., O.R.S.; Writing - review & editing: A.W., K.A., N.J.C., R.M., J.B.-M., O.R.S.; Visualization: A.W.; Supervision: O.R.S.; Project administration: A.W., O.R.S.

Funding

This study was funded by the Norwegian School of Sport Sciences.

References

- Azizi, E. and Roberts, T. J. (2014). Geared up to stretch: pennate muscle behavior during active lengthening. *J. Exp. Biol.* **217**, 376–381.
- Azizi, E., Brainerd, E. L. and Roberts, T. J. (2008). Variable gearing in pennate muscles. *Proc. Natl. Acad. Sci. USA* **105**, 1745–1750.
- Bell, A. L., Brand, R. A. and Pedersen, D. R. (1989). Prediction of hip joint centre location from external landmarks. *Hum. Mov. Sci.* **8**, 3–16.
- Cronin, N. J., Carty, C. P., Barrett, R. S. and Lichtwark, G. (2011). Automatic tracking of medial gastrocnemius fascicle length during human locomotion. *J. Appl. Physiol.* **111**, 1491–1496.
- Cronin, N. J., Avela, J., Finni, T. and Peltonen, J. (2013). Differences in contractile behaviour between the soleus and medial gastrocnemius muscles during human walking. *J. Exp. Biol.* **216**, 909–914.
- Farris, D. J. and Lichtwark, G. A. (2016). UltraTrack: software for semi-automated tracking of muscle fascicles in sequences of B-mode ultrasound images. *Comput. Methods Programs Biomed.* **128**, 111–118.
- Farris, D. J., Lichtwark, G. A., Brown, N. A. T. and Cresswell, A. G. (2016). The role of human ankle plantar flexor muscle–tendon interaction and architecture in maximal vertical jumping examined in vivo. *J. Exp. Biol.* **219**, 528.
- Fukunaga, T., Kubo, K., Kawakami, Y., Fukashiro, S., Kanehisa, H. and Maganaris, C. N. (2001). In vivo behaviour of human muscle tendon during walking. *Proc. R. Soc. Lond. B. Biol. Sci.* **268**, 229–233.
- Griffiths, R. I. (1991). Shortening of muscle fibres during stretch of the active cat medial gastrocnemius muscle: the role of tendon compliance. *J. Physiol.* **436**, 219–236.
- Guilhem, G., Doguet, V., Hauraix, H., Lacourpaille, L., Jubeau, M., Nordez, A. and Dorel, S. (2016). Muscle force loss and soreness subsequent to maximal

- eccentric contractions depend on the amount of fascicle strain in vivo. *Acta Physiol.* **217**, 152–163.
- Hawkins, D. and Hull, M. L.** (1990). A method for determining lower extremity muscle-tendon lengths during flexion/extension movements. *J. Biomech.* **23**, 487–494.
- Hermens, H. J., Freriks, B., Disselhorst-Klug, C. and Rau, G.** (2000). Development of recommendations for SEMG sensors and sensor placement procedures. *J. Electromyogr. Kinesiol.* **10**, 361–374.
- Ishikawa, M., Niemelä, E. and Komi, P. V.** (2005). Interaction between fascicle and tendinous tissues in short-contact stretch-shortening cycle exercise with varying eccentric intensities. *J. Appl. Physiol.* **99**, 217–223.
- Katz, B.** (1939). The relation between force and speed in muscular contraction. *J. Physiol.* **96**, 45–64.
- Kawakami, Y., Muraoka, T., Ito, S., Kanehisa, H. and Fukunaga, T.** (2002). In vivo muscle fibre behaviour during counter-movement exercise in humans reveals a significant role for tendon elasticity. *J. Physiol.* **540**, 635–646.
- Konow, N. and Roberts, T. J.** (2015). The series elastic shock absorber: tendon elasticity modulates energy dissipation by muscle during burst deceleration. *Proc. R. Soc. Lond. B. Biol. Sci.* **282**, 20142800.
- Konow, N., Azizi, E. and Roberts, T. J.** (2012). Muscle power attenuation by tendon during energy dissipation. *Proc. R. Soc. Lond. B. Biol. Sci.* **279**, 1108.
- Kristianslund, E., Krosshaug, T. and van den Bogert, A. J.** (2012). Effect of low pass filtering on joint moments from inverse dynamics: implications for injury prevention. *J. Biomech.* **45**, 666–671.
- Kurokawa, S., Fukunaga, T. and Fukashiro, S.** (2001). Behavior of fascicles and tendinous structures of human gastrocnemius during vertical jumping. *J. Appl. Physiol.* **90**, 1349–1358.
- Lichtwark, G. A. and Wilson, A. M.** (2005). In vivo mechanical properties of the human Achilles tendon during one-legged hopping. *J. Exp. Biol.* **208**, 4715–4725.
- Lichtwark, G. A. and Wilson, A. M.** (2006). Interactions between the human gastrocnemius muscle and the Achilles tendon during incline, level and decline locomotion. *J. Exp. Biol.* **209**, 4379–4388.
- Maharaj, J. N., Cresswell, A. G. and Lichtwark, G. A.** (2016). The mechanical function of the tibialis posterior muscle and its tendon during locomotion. *J. Biomech.* **49**, 3238–3243.
- Raiteri, B. J., Cresswell, A. G. and Lichtwark, G. A.** (2016). Three-dimensional geometrical changes of the human tibialis anterior muscle and its central aponeurosis measured with three-dimensional ultrasound during isometric contractions. *PeerJ* **4**, e2260.
- Roberts, T. J.** (2016). Contribution of elastic tissues to the mechanics and energetics of muscle function during movement. *J. Exp. Biol.* **219**, 266–275.
- Roberts, T. J. and Azizi, E.** (2010). The series-elastic shock absorber: tendons attenuate muscle power during eccentric actions. *J. Appl. Physiol.* **109**, 396–404.
- Roberts, T. J. and Azizi, E.** (2011). Flexible mechanisms: the diverse roles of biological springs in vertebrate movement. *J. Exp. Biol.* **214**, 353–361.
- Spanjaard, M., Reeves, N. D., van Dieën, J. H., Baltzopoulos, V. and Maganaris, C. N.** (2007). Gastrocnemius muscle fascicle behavior during stair negotiation in humans. *J. Appl. Physiol.* **102**, 1618–1623.
- Spanjaard, M., Reeves, N. D., van Dieën, J. H., Baltzopoulos, V. and Maganaris, C. N.** (2008). Lower-limb biomechanics during stair descent: influence of step-height and body mass. *J. Exp. Biol.* **211**, 1368–1375.
- Tilp, M., Steib, S. and Herzog, W.** (2012). Length changes of human tibialis anterior central aponeurosis during passive movements and isometric, concentric, and eccentric contractions. *Eur. J. Appl. Physiol.* **112**, 1485–1494.